Mammalian Biology
https://doi.org/10.1007/s42991-019-00001-0

ORIGINAL ARTICLE

Phylogeography of the striped field mouse, *Apodemus agrarius* (Rodentia: Muridae), throughout its distribution range in the Palaearctic region

Alice Latinne[1,2] · Miguel Navascués[3,4] · Marina Pavlenko[5] · Irina Kartavtseva[5] · Rainer G. Ulrich[6] · Marie-Laure Tiouchichine[1] · Gilles Catteau[1] · Hela Sakka[1] · Jean-Pierre Quéré[3] · Galina Chelomina[5] · Aleksey Bogdanov[7] · Michal Stanko[8] · Lee Hang[9] · Karsten Neumann[10] · Heikki Henttonen[11] · Johan Michaux[1,12]

Received: 27 August 2019 / Accepted: 19 November 2019

Abstract

To better understand the evolutionary history of oriental wildlife newcomers in Europe, we studied the phylogeography and demographic history of the striped field mouse, *Apodemus agrarius*, throughout its Palaearctic distribution area. Genetic datasets including cytochrome b gene sequences and microsatellite markers were analysed using a large range of population genetics methodologies, including coalescent models and approximate Bayesian computations. Our results showed high mitochondrial genetic homogeneity among *A. agrarius* populations throughout the Palaearctic region, but microsatellite markers detected a finer population structure with the genetic differentiation of populations from the Eastern and Western distribution ranges. The Western colonisation likely originated from Far East Russian populations during one of the last interglacials. After their colonisation of the Central Asia and Western regions, the Central Palaearctic populations became isolated from their Eastern relatives. Our coalescent-based approaches suggested a separation between these two distribution ranges around 38 kya or more recently (around 11 kya). Limited gene flow still happened between populations in the two main distribution ranges, mainly from the Eastern to Western populations. Our study, for the first time, provides an overview of the evolutionary and demographic history of the striped field mouse throughout the Palaearctic region. *A. agrarius* appears to be an Asiatic immigrant and a relatively new member of the European fauna community. This study further confirms the important role of Far East Asian regions as a source of European biodiversity.

Keywords Glacial refugia · Palaearctic region · *Apodemus agrarius* · Continental colonisation

Introduction

Quaternary climatic oscillations have played a major role in shaping the present geographical distribution and structuring the genetic diversity of numerous species. In the Northern Hemisphere, this resulted in the extinction of northern populations during ice ages, followed by northward expansion from refugia during interglacial periods (Hewitt, 2000). Refugial areas for European small mammals were mainly located in the Mediterranean, Ural and Caucasus/Carpathian regions (Deffontaine et al. 2009; Herman et al. 2016; Lalis et al. 2016; Michaux et al. 2003). However, some other authors have also proposed that much more northern regions such as Western Scandinavia, Southern Great Britain or the Baltic area would have also provided additional refuges for some boreal as well as temperate mammal species (Ruiz-González et al. 2013; Stewart and Dalén, 2008); but this hypothesis has been strongly debated and now appears unlikely (Hughes et al. 2016). Europe was also recolonised by some species from Central Asian refugia after the last glacial maximum, i.e. voles *Myodes glareolus* (Deffontaine et al. 2005); *Microtus agrestis* (Herman et al. 2014); *Microtus arvalis* (Sibiryakov et al. 2018); or the wood lemming, *Myopus schisticolor* (Fedorov et al. 2008).

Handling editor: Allan McDevitt.

Electronic supplementary material The online version of this article (https://doi.org/10.1007/s42991-019-00001-0) contains supplementary material, which is available to authorized users.

✉ Johan Michaux
johan.michaux@uliege.be

Extended author information available on the last page of the article

Published online: 21 January 2020

Finally, a few mammal species probably colonised Europe from much farther regions, such as the Russian Far East or China, e.g. the common hamster, *Cricetus cricetus* (Neumann et al. 2005) and the harvest mouse, *Micromys minutus* (Yasuda et al. 2005). However, many questions regarding the relationships between populations from Eastern and Western Palaearctic areas also remain unanswered: Where did they survive during the Quaternary glaciations? How and when did the oriental populations colonise the Western regions? To gain further insight into the genetic structure of oriental wildlife newcomers in Europe, we studied the phylogeography and demographic history of the striped field mouse, *Apodemus agrarius* (Pallas, 1771), throughout its distribution area. This species is widely distributed over the entire Palaearctic region, from Central Europe to the Korean Peninsula and Russian Far East. However, its distribution range is divided into two separate fragments (Europe–Western Siberia and Russian Far East–China), which are about

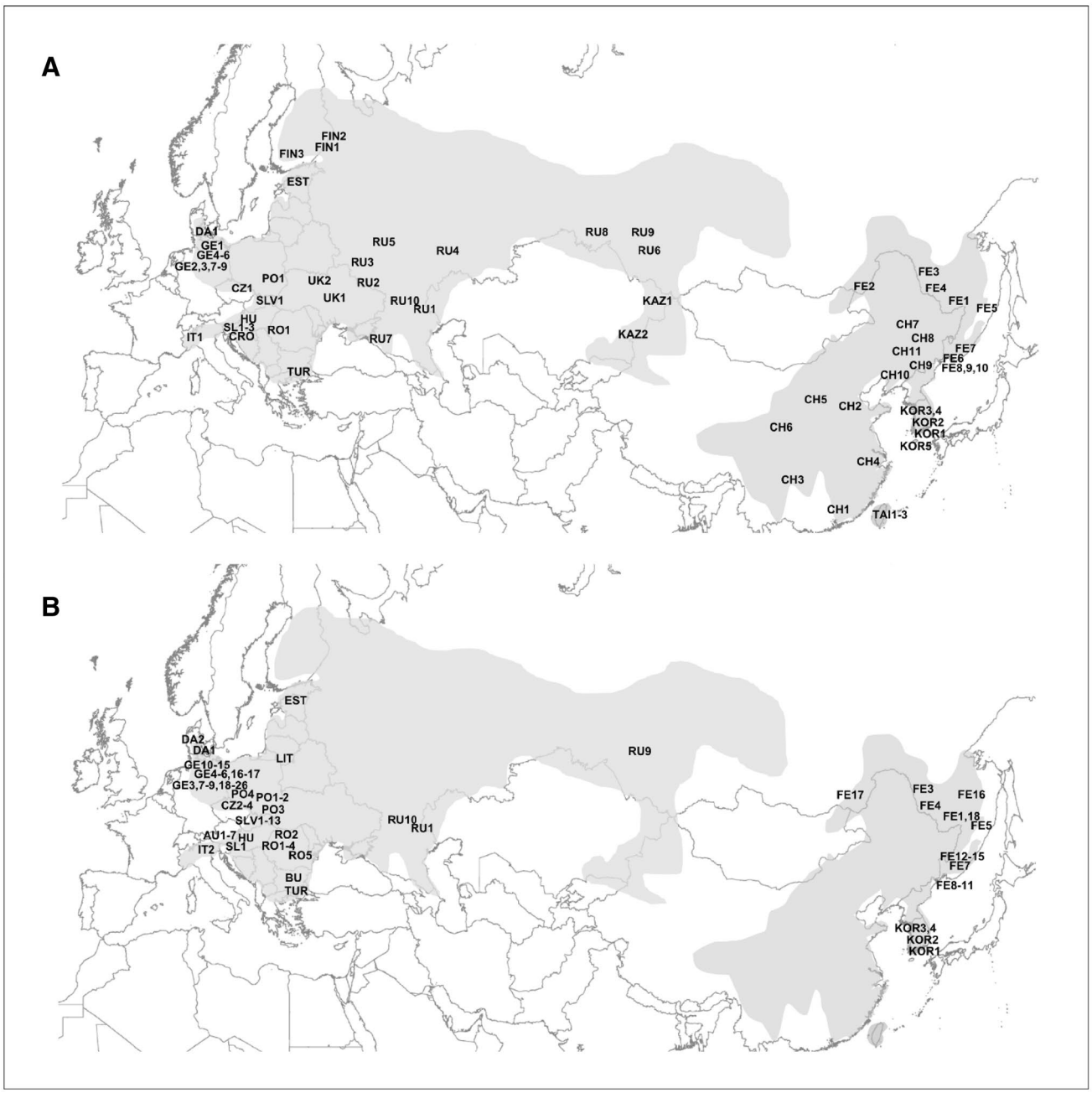

Fig. 1 Distribution range of *Apodemus agrarius* (shaded area) and sampling localities of mitochondrial (**a**) and microsatellite (**b**) datasets. The locality codes are given in Table 1

600–700 km apart, with the disjunction zone running along Transbaikalia and Mongolia (Fig. 1). Although some parts of this disjunction zone seem to be presently colonised by the species due to recent human activities and introductions (Bazhenov et al. 2015), there is currently no permanent contact between *A. agrarius* populations from both fragments.

Apodemus agrarius is a host of the Hantaan virus in the Far East and China, and of Kurkino and Saaremaa strains of the Dobrava hantavirus in the Western Palaearctic, which causes haemorrhagic fever with renal syndrome (HFRS) in humans (Klempa et al. 2013; Xiao et al. 2018). This species also serves as a reservoir of pathogenic *Leptospira*, *Rickettsia*, *Orientia* and *Bartonella* bacteria (Fischer et al. 2018; Gajda et al. 2017; Kraljik et al. 2016). Greater knowledge of its evolutionary history and genetic diversity is therefore also important to gain insight into its colonisation dynamics and therefore the risks of disease transmissions in new areas.

Most phylogeographic studies of *A. agrarius* have focused on a small part of its distribution range (Andersen et al. 2017; Gortat et al. 2013; Koh et al. 2014; Pereverzeva et al. 2017; Sheremetyeva et al. 2017), but phylogeographic information from datasets including samples from the two main population fragments and based on karyotype variations (Kartavtseva and Pavlenko, 2000) or random amplified polymorphic DNA (RAPD) markers (Atopkin et al. 2007) has shown very weak genetic differences among animals from the two fragments, but the Eastern group nevertheless seems to be more heterogeneous than the Western group. These findings were confirmed by another study based on mitochondrial cytochrome *b* gene (MTCYB) sequences (Sakka et al. 2010). The low karyotype and allozyme differentiation in the striped field mouse suggest a recent and rapid spread of the species from the Eastern to the Western Palaearctic (Atopkin et al. 2007; Kartavtseva and Pavlenko 2000). However, this hypothesis would need to be confirmed by better sampling throughout the species' distribution range as well as by the use of more sensitive genetic methods based on rapidly evolving markers. The present study was carried out to better understand the phylogeographic structure and demographic history of the striped field mouse from the species' two main distribution areas using mitochondrial MTCYB gene sequencing and microsatellite marker genotyping. Further investigation of the demographic history of the striped field mouse using recent statistical methods based on the coalescent theory will also be useful to gain greater insight into the demographic and expansion history of this species.

Materials and methods

Samples and MTCYB gene amplification

A total of 158 *A. agrarius* individuals were sequenced for the MTCYB gene. All samples used in the present study were tissue (ear or liver) samples stored in ethanol. These specimens were obtained from our network of collaborators, museum collections and field trips performed by our laboratories. Animals were treated in accordance with the guidelines of the American Society of Mammalogists, and within the European Union legislation guidelines (Directive 86/609/EEC).

Genomic DNA was extracted using the DNeasy™ Tissue kit (Qiagen Inc., Valencia, CA) according to the manufacturer's instructions. The MTCYB gene was amplified using the universal PCR primers L7 (5′-ACCAATGACATGAAAAATCATCGTT-3′) and H16 (5′-ACATGAATYGGAGGY-CAACCWG-3′) (Kocher et al. 1989). Amplifications were carried out according to the protocol of Michaux et al. (2003) and performed in a Labover PTC100 thermal cycler through 39 cycles (30 s/94 °C, 1 min/52 °C, 2 min/68 °C) with a final 10 min extension cycle at 68 °C. All sequencing procedures were performed by Macrogen Inc. (Seoul, South Korea). The sequences were aligned using the ClustalW algorithm in BIOEDIT 7.0.5.2 (Hall, 1999). Twenty-four MTCYB sequences from *A. agrarius* available in GenBank were also added to this dataset to cover the entire *A. agrarius* distribution range (68 localities in 20 countries) (Table 1 and Fig. 1; Table A.1).

Microsatellite genotyping

We also genotyped 340 *A. agrarius* specimens from 88 localities in 17 countries using nine microsatellite markers (Table 1 and Fig. 1; Table A.1) selected from Makova et al. (1998) according to their amplification protocol. Reaction mixtures contained approximately 100 ng of genomic DNA, 2.5 units of Taq DNA polymerase (Promega), 10 units of Promega buffer, 1.5 mM of $MgCl_2$, 0.6 mM of each primer (labelled and unlabelled), 250 mM of dNTPs (Perkin Elmer) and water to achieve a final volume of 25 µL. The thermal conditions included an initial 3 min denaturation step at 94 °C, followed by 35 cycles (1 min/94 °C, 30–45 s/annealing temperature, 30–60 s/72 °C) and a final 3 min extension at 72 °C. After amplification, the nine microsatellite loci were combined in two multiplexes for each animal and analysed on an ABI 3100 automatic sequencer. The results were compiled and analysed with the GeneScanTM and GenotyperTM software packages (ABI).

Table 1 Number and geographic origin of *A. agrarius* samples used in this study

Country	MTCYB dataset		Microsatellite dataset	
	Number of sequences	Number of localities	Number of genotyped individuals	Number of localities
Austria			21	7 (AU1-7)
Bulgaria			8	1 (BU)
China	29	11 (CH1-11)		
Croatia	5	1 (CRO)		
Czech Republic	4	1 (CZ1)	10	3 (CZ2-4)
Denmark	5	1 (DA1)	19	2 (DA1-2)
Estonia	1	1 (EST)	1	1 (EST)
Finland	3	3 (FIN1-3)		
Germany	10	9 (GE1-9)	61	24 (GE3-26)
Hungary	2	1 (HU)	2	1 (HU)
Italy	1	1 (IT1)	1	1 (IT2)
Kazakhstan	3	2 (KAZ1-2)		
Lithuania			1	1 (LIT)
Poland	5	1 (PO1)	31	4 (PO1-4)
Romania	4	1 (RO1)	11	5 (RO1-5)
Russia (Far East)	52	10 (FE1-10)	68	16 (FE1, FE3-5, FE7-18)
Russia (European part + Siberia)	19	10 (RU1-10)	13	3 (RU1, RU9-10)
Slovakia	1	1 (SLV1)	79	13 (SLV1-13)
Slovenia	6	3 (SL1-3)	1	1 (SL1)
South Korea	18	5 (KO1-5)	12	4 (KO1-4)
Taiwan	9	3 (TAI1-3)		
Turkey	3	1 (TUR)	1	1 (TUR)
Ukraine	2	2 (UK1-2)		

Mitochondrial data analysis

The final MTCYB dataset included 182 sequences from *A. agrarius*. Phylogenetic reconstructions were performed using the maximum-likelihood criterion (ML) algorithm implemented in PHYML (Guindon et al. 2010) and two *Apodemus chevrieri* haplotypes as outgroups. We used jMODELTEST (Posada 2008) to determine the most suitable DNA substitution model for the MTCYB dataset studied. The robustness of the tree was assessed by 1000 bootstrap resamplings. A median-joining network was constructed using NETWORK 4.5 software (Bandelt et al. 1999).

Haplotype (h) and nucleotide (π) diversities, Fu's *F*s and population pairwise F_{ST} were estimated using ARLEQUIN 3.5 (Excoffier and Lischer 2010). These indices were calculated for the Eastern ($n = 108$) and Western Palaearctic groups ($n = 74$).

Demographic histories of the two main striped field mouse groups (Eastern and Western Palaearctic groups) were inferred using our MTCYB gene dataset and an isolation-with-migration (IM) model implemented in the IM program (Hey and Nielsen 2004). The model uses coalescent simulation within a Bayesian inference framework to estimate posterior probability distributions for five parameters, including: contemporary and ancestral effective population sizes ($\theta = 2N_e\mu$), divergence times ($T = t\mu$) and rates of gene flow between the Eastern and Western fragments. We assumed an HKY model of sequence evolution (Hasegawa et al. 1985) and equal migration rates in both directions (i.e. just one migration parameter, *m*). However, the effective number of migrants ($2N_em$) from each population can differ as θ estimates differed between Eastern and Western Palaearctic groups. We used a burn-in of 200,000 steps followed by a run of 1 million steps. To ensure reliable convergence towards the stationary distribution, we monitored multiple independent runs, each with 70–100 independent chains under Metropolis coupling, to improve mixing. Mixing properties of the Markov-chain Monte-Carlo method (MCMC) were assessed by examining the level of autocorrelation between the final and initial parameter values and by visual inspection of the parameter trend plots. The analyses were considered to have converged upon the stationary distribution if independent runs generated similar posterior distributions, with each having at least an effective sample size of 100 for each estimated parameter.

To convert the parameter estimates scaled by μ (i.e. T and θ) to demographic units, we used two mutation rates available in the literature: a mutation rate of $1.1–1.7\times10^{-7}$ mutation/site/year proposed by Suzuki et al. (2015) and a mutation rate of $1.8–3.9\times10^{-7}$ mutation/site/year from Andersen et al. (2017). However, as this last estimate was calculated for another rodent genus (*Mus musculus*) from very recent events (200 years), it has to be used with caution. Assuming a generation time (G) for *A. agrarius* of 0.5 year (Pereverzeva et al. 2017), the population divergence time (T) can be converted to calendar years (t in years) and estimates of population mutation rates (θ_1, θ_2, and θ_A) can be converted to estimates of effective population size parameters (N_1, N_2, N_A, respectively, in number of individuals). The migration parameters in the model can be used to obtain population migration rates (i.e. the effective number of migrants per generation), using an estimate of θ (i.e. $2Nm=\theta m/2$) (Fontaine et al. 2010). $2N_1m$ and $2N_2m$ are the effective number of migrants per generation in populations 1 and 2, respectively.

Microsatellite data analysis

The proportion of null alleles (NA) at each locus and for each population was estimated with FREENA (Chapuis and Estoup 2007). Genetic diversity was assessed by calculating the expected (He) and observed (Ho) heterozygosities with ARLEQUIN over all loci for each group and Hardy–Weinberg equilibrium (HWE) was tested using GENEPOP (Rousset 2008). Multi-locus F_{IS} was calculated for each group with FSTAT 2.9.3.2 (Goudet 2001). The allelic richness (AR) was calculated using the rarefaction procedure implemented in FSTAT.

STRUCTURE 2.3.1 (Pritchard et al. 2000) was used to infer the number of populations (K) and assign individuals to genetic clusters independently of spatial sampling. Ten iterations were run for each K value from 1 to 15 using an admixture model with a burn-in of 1×10^5 and MCMC values of 1×10^6. We used CLUMPAK (Kopelman et al. 2015) to average the results of multiple iterations for a given K.

The demographic history of *A. agrarius* was also inferred from microsatellite data using an approximate Bayesian computation (ABC) approach via a random forest algorithm (Raynal et al. 2019; Pudlo et al. 2016) performed with microsatABC-IM (Navascués 2017). ABC uses a coalescent model to generate a reference panel of simulations that are compared to real data based on summary statistics. Simulated datasets more similar to the real data are considered to be generated by models with higher likelihood. This comparison between simulated and real data is done using a random forest algorithm. Forty thousand simulations were generated to create the reference table and random forests of 1000 trees were used for the parameter and posterior probability estimation.

A model of two populations (Eastern and Western clusters) was evaluated. Each population was characterised by a parameter θ ($\theta_W=4N_W\mu$ and $\theta_E=4N_E\mu$, where N_W is the effective population size of the Western population ($n=260$), N_E is the effective population size of the Eastern population ($n=80$), and μ is the mutation rate). The Western population was separated from the Eastern population at time $T=t/4N_W$ (time t measured in number of generations). Two concurrent models were evaluated regarding the presence or absence of gene flow between the two populations. If gene flow was detected, an additional parameter, i.e. the scaled migration rate $M=4N_Wm$, was included. Microsatellites were assumed to mutate according to a generalised stepwise mutation model (GSM) in which the number of repeat units gained or lost in each mutation is taken from a geometric distribution with parameter P_{GSM}. Data under this model were generated by simulation using coalescent simulator ms (Hudson 2002) with a custom script (see below) to transform its output into microsatellite data. Each simulated dataset was summarised on the basis of population genetics statistics to characterise microsatellite genetic diversity and population differentiation, which are known to be informative about demographic patterns (Table A.2). Parameter values

Table 2 Parameters (coalescent scale) estimated for the isolation using the migration model in our approximate Bayesian computations: scaled effective population sizes of the Western population (θ_W) and Eastern population (θ_E); foundation time of Western population (T); migration rate (M); and geometric parameter for the generalised stepwise mutation model (P_{GSM})

	Prior	Prior MSE	Median	95% HPD
θ_W	Log uniform (0.1, 1000)	1.30	5.25	1.86–81.69
θ_E	Log uniform (0.1, 1000)	1.05	11.86	6.70–164.53
T	Log-uniform (10^{-5}, 10)	1.67	0.17	0.03–8.45
M	Log uniform (10^{-5}, 100)	973.82	4.96×10^{-3}	1.24×10^{-5}–3.64
P_{GSM}	Uniform (0, 1)	6.39×10^{-3}	0.50	0.09–0.64

MSE mean squared error

at each simulation were sampled from uninformative prior probability distributions covering a wide range of values (Table 2). To convert the parameter estimates from the ABC analysis scaled by μ (i.e. T and θ) to demographic units, we used an estimate of N_W obtained from θ_W point estimate, a generation time of 0.5 year and a microsatellite mutation rate estimated for *M. musculus* (5×10^{-5} per generation, Dietrich et al. 1992) as no estimate of mutation rate is available for *A. agrarius*.

Results

Mitochondrial DNA analysis

Phylogenetic and phylogeographic analysis

A total of 121 haplotypes of 923 base pairs (bps) were identified within our MTCYB dataset (Table A.3). All new sequences have been deposited in GenBank (accession numbers MH257777–MH257893). ML analyses were performed using the HKY85 + I + Gamma model estimated using jModelTest.

Three main lineages were recovered in the ML phylogenetic tree (Fig. A.1). The first two lineages to diverge were well supported and included all haplotypes from Jeju Island in South Korea (BS = 83%) and Taiwan (BS = 94%), respectively. The third lineage was weakly supported (BS = 20%) and did not show any clear phylogeographic structure. Haplotypes corresponding to animals coming from the whole distribution area were mixed in this lineage and not associated with any supported clades (Fig. A.1). Similarly our median-joining network showed a lack of clear phylogeographic structure (Fig. 2). Interestingly, some MTCYB haplotypes are shared among individuals from Russian Far East and Europe, from Europe and Central Russia and from Western Siberia and Central Russia.

Analysis of genetic diversity and differentiation

Populations from within the Western Palaearctic range were characterised by lower nucleotide diversity values (from 0.0062) as compared to those within the Eastern Palaearctic range (0.0159) (Table 3). Findings of Fu's *F*s test of neutrality were significant for both groups ($p < 0.05$) (Table 3), which indicated population expansion. High F_{ST} estimates (> 0.20) confirmed strong genetic differentiation between the Eastern and Western subgroups.

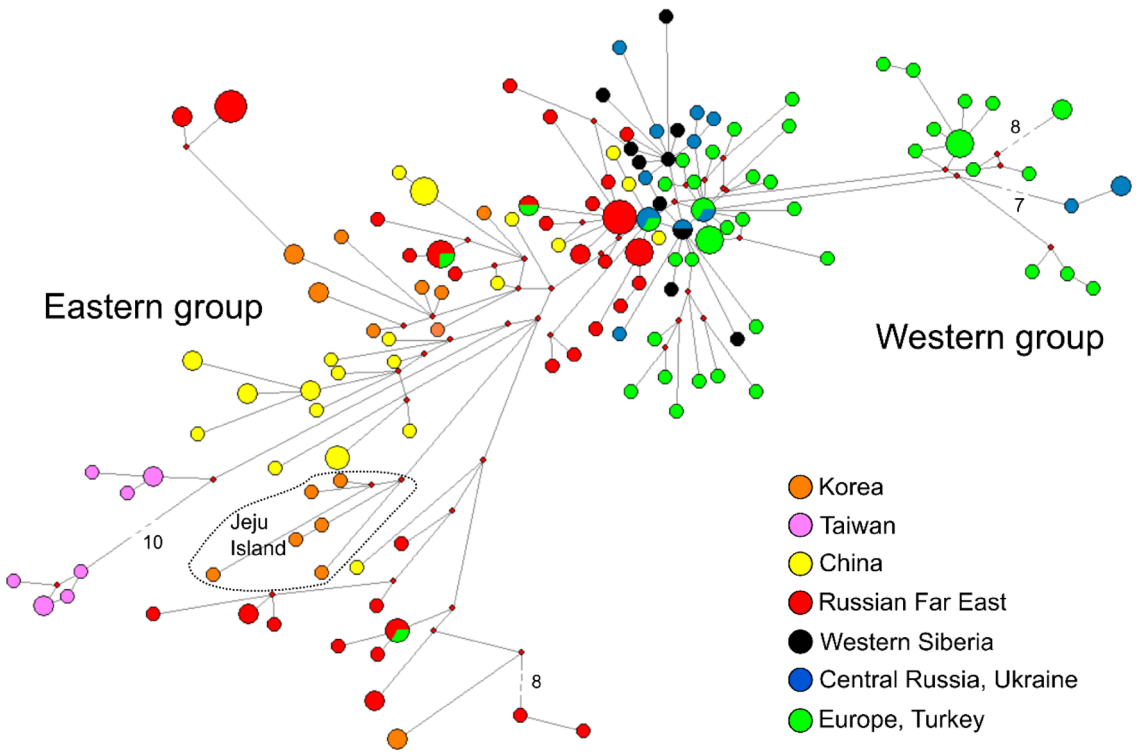

Fig. 2 Median-joining network based on the MTCYB dataset. Circles correspond to distinct haplotypes and circle sizes are proportional to the number of animals sharing this haplotype. Branch lengths are proportional to the number of mutations between haplotypes, unless indicated otherwise

Table 3 Diversity estimates for *A. agrarius* groups: haplotype (h) and nucleotide (π) diversities and their standard deviation and Fu's *F*s values

	Corresponding localities	*N*	$h \pm$ SD	$\pi \pm$ SD	Fu's *F*s
Overall	All	182	0.9933 ± 0.0016	0.0135 ± 0.0068	**− 24.05267**
Eastern group	CH1-11, TAI1-3, KO1-5, FE1-10	108	0.9894 ± 0.0033	0.0159 ± 0.0079	**− 24.10376**
Western group	CRO, CZ1, DA1, EST, FIN1-3, GE1-9, HU, IT1, PO1, RO1, SLV1, SL1-3, TUR, RU1-10, UK1-2, KAZ1-2	74	0.9874 ± 0.0056	0.0062 ± 0.0034	**− 25.48372**

Significant Fu's *F*s values are indicated in bold ($p < 0.05$)

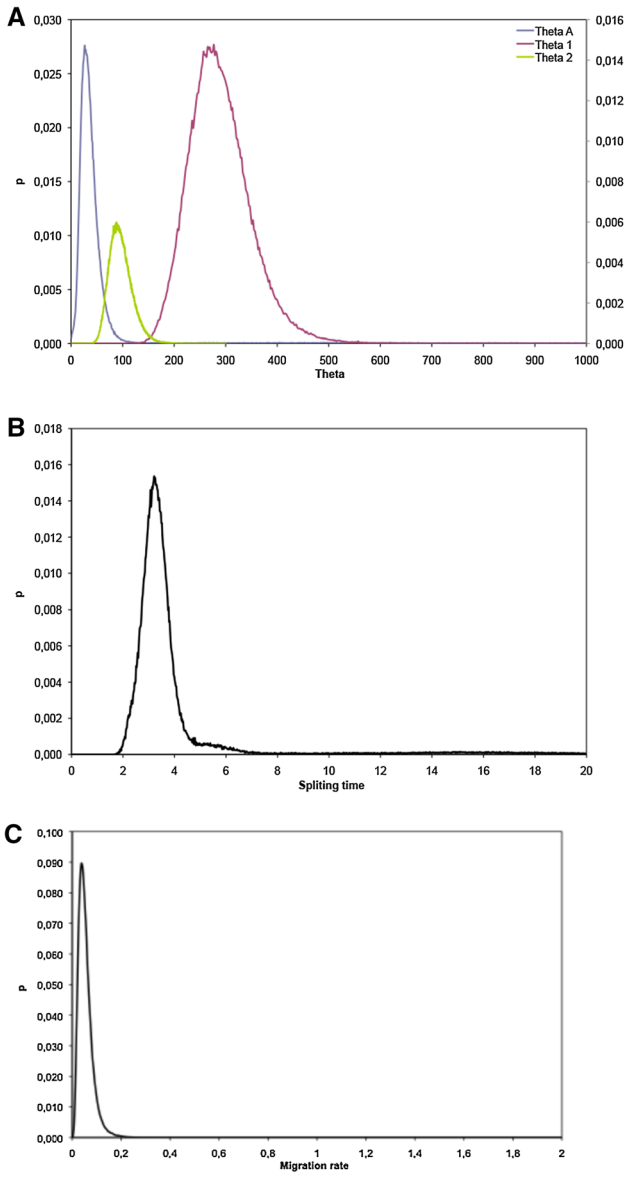

Fig. 3 Plots of posterior probability of parameters estimated with the isolation-with-migration model (scaled by the mutation rate μ): **a** Effective population sizes of the Eastern lineage (θ_1), Western lineage (θ_2) and ancestral population (θ_A), **b** splitting time between Eastern and Western lineages and **c** migration rate (m) between Eastern and Western lineages

Demographic history (IM model)

The estimated current population size of the Eastern lineage was threefold larger than that of the Western lineage (Fig. 3 and Table 4). The divergence time between these two lineages was estimated at 38 kya (95% highest posterior density, HPD: 28–50 kya) under the IM model and the rate proposed by Suzuki et al. (2015). The divergence time estimated using the rate from Andersen et al. (2017) was more recent (10.6 kya; 95% HPD: 7.8–14 kya) (Table 4). Gene flow was estimated at around 4.4 female migrants per generation from East to West and 1.4 migrant per generation from West to East.

Microsatellite data analysis

Genetic diversity

The NA frequency values determined in FreeNA were very low for each locus in each group. The observed heterozygosity and allelic richness were higher in the Eastern group (Table 5). Tests for HWE showed deviation from the expected frequencies in both groups. Inbreeding coefficients (*F*is) were significant ($p < 0.05$) (Table 5).

Population structure

We used the ΔK method described by Evanno et al. (2005) to interpret the STRUCTURE output. The highest ΔK was found at $K = 2$ (Fig. A.2). For $K = 2$, the Korean populations clustered with populations from the Russian Far East (Eastern group) (Fig. 4). The second cluster corresponded to the Western group (European, Turkish, Russian, Ukrainian and Kazakh populations). The Eastern cluster (Korea + Russian Far East) was recovered until $K = 5$ (Fig. A.3).

Demographic history

Distinguishing between models was difficult; the model with migration between Western and Eastern populations was marginally favored over a model of pure divergence with a posterior probability estimated at only 0.54. High rates of historical migration were rejected (Fig. A.4.), suggesting strong separation between the two groups despite the occasional admixed individuals. Because of this low posterior

Table 4 Modes (and 95% HPD) of parameters estimated with the isolation-with-migration model and the MTCYB dataset and converted to a demographic scale assuming a mutation rate of 11%/Myr (Suzuki et al. 2015) or 39%/Myr (Andersen et al. 2017), and a generation time of 0.5 year

MTCYB mutation rate	11%/Myr	39%/Myr
Divergence time *t* (years)	37,621 (27,652–50,201)	10,611 (7799–14,159)
Population size Eastern group (number of individuals)	1,608,117 (1,169,000–2,225,255)	453,571 (329,718–627,636)
Population size Western group (number of individuals)	515,665 (350,106–759,553)	145,444 (98,748–214,233)
Ancestral population size (number of individuals)	163,185 (56,373–376,809)	46,026 (15,900–106,279)
Number of migrants from Eastern group	4.4 (1.2–19.2)	4.4 (1.2–19.2)
Number of migrants from Western group	1.4 (0.4–6.6)	1.4 (0.4–6.6)

The length of the usable sequence was 766 bps

Table 5 Microsatellite genetic diversity within *A. agrarius* groups: observed (Ho) and expected (He) heterozygosities, inbreeding coefficient (*F*is) and allelic richness (AR)

	Corresponding localities	*n*	Ho	He	*F*is	AR
Overall	All	340	0.6763 ± 0.1235	0.8064 ± 0.1030	**0.162**	21.07
Eastern group	KO1-4, FE1, FE3-5, FE7-18	80	0.7327 ± 0.1084	0.86524 ± 0.0569	**0.109**	16.66
Western group	AU1-7, BU, CZ2-4, DA1-2, EST, GE3-26, HU, IT2, LIT, PO1-4, RO1-5, SLV1-13, SL1, TUR, RU1, RU9-10	260	0.6589 ± 0.1538	0.739 ± 0.1659	**0.154**	12.61

Significant values are indicated in bold ($p < 0.05$)

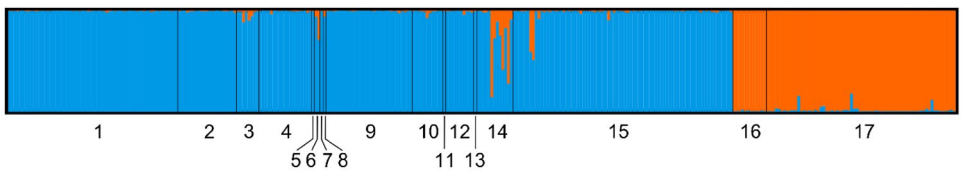

Fig. 4 Population structure estimated using STRUCTURE ($K = 2$). Each individual is represented by a vertical line partitioned into K colour segments, with the length of each colour segment being proportional to the estimated membership coefficient. Numbers correspond to the sampling countries: 1 = Germany, 2 = Austria, 3 = Bulgaria, 4 = Denmark, 5 = Estonia, 6 = Hungary, 7 = Italy, 8 = Lithuania, 9 = Poland, 10 = Romania, 11 = Slovenia, 12 = Czech Republic, 13 = Turkey, 14 = Russia (Central Russia + Siberia), 15 = Slovakia, 16 = South Korea, 17 = Russian Far East

Table 6 Median (and 95% HPD) of parameters estimated using the microsatellite dataset and an approximate Bayesian computation and converted on a demographic scale assuming a mutation rate of 5×10^{-5} per generation and a generation time of 0.5 year

	Median (and 95% HPD)
Divergence time t (years)	8925 (1575–443,625)
Population size Eastern group (number of individuals)	59,300 (33,500–822,650)
Population size Western group (number of individuals)	26,250 (9,300–408,450)
Number of migrants from Eastern group	4.72×10^{-8} (1.18×10^{-10}–3.47×10^{-5})

probability, parameters common to both models were estimated from the reference table for both models. The migration rate was also estimated for the isolation-with-migration model. Point estimates (median of posterior probability distribution) and 95% HPD intervals are reported in Table 2 and a more detailed description of the posterior distribution is presented in Fig. A.4. Parameter estimates converted to a demographic scale are presented in Table 6. The estimated effective population size of the Eastern group (θ_E) was 2.25-fold higher than that of the Western group (θ_W) (Table 6). The divergence time between these two groups was estimated at 9 kya (95% HPD: 1575–443,625) (Table 6), similar to the divergence time estimated for the MTCYB with IM model and fastest evolution rate (Table 4).

Discussion

Origin and colonisation history of *Apodemus agrarius*

Our results showed high mitochondrial genetic homogeneity among *A. agrarius* populations throughout the Palaearctic region, but microsatellite markers—which mutate more rapidly—detected a finer population structure with the genetic differentiation of populations from the Eastern and Western distribution ranges. These findings suggest a recent separation between the *A. agrarius* groups, with low gene flow among them.

Striped field mouse populations in the Eastern range were characterised by higher genetic diversity than those in the Western range, which confirmed that the species originated in Eastern Asia, likely around 800 kya (Suzuki et al. 2008). The origin of *A. agrarius* in Eastern Asia was also corroborated by our estimates of effective population size for both MTCYB sequences and microsatellites, which highlighted a population size around threefold higher in the Eastern part of the range as compared to the Western part. The lower genetic diversity of Western populations could be the result of founder events associated with a low number of colonisers coming from the East, followed by a recent population expansion in the West. This Western colonisation likely originated from Far East Russian populations as the median-joining network showed closer relationships and shared haplotypes between these two populations. Western colonisation via China appears unlikely as substantial biogeographic barriers, such as the Himalayan Mountains or the Gobi Desert, have hemmed in this region for several million years. The Western colonisation from the Russian Far East could have happened during one of the last interglacials (e.g. the Mindell-Riss or the Riss-Würm interglacials), when warmer climatic conditions would have given rise to a mosaic of forests, meadows, bushes and forest-steppe grasslands in the Transbaikalia region (Batuyev et al. 2000; Velichko 2009). Indeed, these habitats correspond to the ecological preference of *A. agrarius*, and this species cannot survive in taiga or tundra habitats (Okulova et al. 2012). From this time, this species was allowed colonising a large part of the Central and Western Palaearctic region. Indeed, several palaeontological studies suggested a first presence of *A. agrarius* in Central Europe around 50 kya (Popov 2017) and in Southwestern France around 19 kya, although the species is now extinct in this latter region (Aguilar et al. 2008).

After their colonisation of the Central Asia and Western regions, the Central Palaearctic populations became isolated from their Eastern relatives. The IM analyses suggested a separation between these two distribution ranges around 38 kya [considering the rate proposed by Suzuki et al. (2015)] or more recently (around 11 kya) following the rate proposed by Andersen et al. (2017). Similarly, the ABC analyses suggested a separation between these two groups around 9 kya. The most recent temporal estimate for the disjunction of the *A. agrarius* range appears similar to those proposed by Atopkin et al. (2007), who estimated that this separation occurred during the Holocene (< 12 kya), and that it was associated with a heavy dry period in this region, which caused the decline and sometimes even the disappearance of trees and shrubs. However, similar climatic events might have also occurred around 38 kya, at the beginning of the Würm Ice Age, which was characterised by particularly cold and dry climates, and would have led to similar isolation (Velichko 2009). Fossil records in the Transbaikalia region indicated that Late Pleistocene was characterised by a faunal transition and the expansion of dry cold steppes and small mammal species associated with this environment (Erbajeva et al. 2013). However, without more fossil data from this last region, it is difficult to conclude when the Central Palaearctic populations became definitively isolated from their Eastern relatives.

From this period, the Central-Western Palaearctic populations (Western group) started to differentiate from the Russian Far East and Chinese populations, even though some gene flow still took place between the isolated ranges, as suggested by MTCYB and microsatellite data. This gene flow seemed to be higher from East to the West than vice versa. Populations of the Western group continued to increase throughout Central Asia and the European and Turkish regions. According to the low levels of nucleotide diversity as well as the sign of recent expansion revealed by Fu's *F*s index, this last expansion throughout Central Asia and Europe would have occurred relatively quickly, possibly when some habitats preferred by the striped field mouse (mixed vegetation with grasslands, bushes, shrubs, mosaic of forests and meadows) were distributed at the interface between taiga and tundra or steppe habitats in a large area of Central Asia during the Riss-Würm interglacial (Velichko 2009). Herbivorous megafauna could also have favored the persistence of such habitats in the region (Bakker et al. 2016). In contrast, the last Ice Age probably enabled *A. agrarius* to expand into Western Europe, as during this period the European deciduous forest was replaced by a mosaic of open habitats and coniferous forests (Fletcher et al. 2010). At the beginning of the Holocene, the striped field mouse distribution range probably regressed from most of Western Europe when deciduous forests started their postglacial recolonisation. This resulted in the species only surviving in Central European open habitats. It is only during recent periods, when human activities created open habitats via agricultural development, that the striped field mouse has been able to recolonise some Western European

regions (Germany, Denmark, Italy, and more recently Austria, Hungary, Slovakia and Czech Republic) (Spitzenberger and Engelberger 2014).

This type of colonisation pattern from Far East Asia is quite rare for mammals. It has probably been facilitated by the high ecological plasticity and synanthropic habits of the striped field mouse. To our knowledge, this pattern has only been observed in the harvest mouse (*M. minutus*) (Yasuda et al. 2005). These latter authors described a close genetic relationship between Western and Eastern Palaearctic *M. minutus* populations and a process of recolonisation of Europe from refugia located in Central and Eastern Asia around 80 kya. A similar pattern has also been reported in roe deer (*Capreolus pygargus*) as populations from Lithuania and Poland appear to be genetically closely related to those from Central and Far East Asia, suggesting recent colonisation of Europe from these Eastern regions (Lorenzini et al. 2014).

Eastern refuge areas

Apodemus agrarius showed a complex genetic structure within the Eastern range. China, the Russian Far East and Korea correspond to important centres of diversification for this species as the genetic diversity levels are higher within these regions as compared to Western regions. This diversification could be the result of repeated population isolation during the Quaternary Ice Ages, which led to allopatric differentiation. During these periods, the cooler climate allowed the extension of the Gobi Desert towards Pacific areas. This in turn probably led to isolation of the Russian Far East (Primorye and Khabarovsk regions) from several Chinese regions (Zhang et al. 2008) as well as from populations in the Korean Peninsula (Koh et al. 2014). The Korean Peninsula, characterised by a temperate mountain climate in its southern part, was less deeply affected by the global Quaternary climate changes (Kim and Park, 2015) and therefore could have acted as glacial refugia for many organisms during the Quaternary coldest phases. The Russian Far East as well as China could also have been a potential Quaternary refugium for *A. agrarius* (Atopkin et al. 2007; Pereverzeva et al. 2017; Sakka et al. 2010).

Taxonomic implication

Corbet (1978) classified *A. agrarius* populations from Europe and Western and Central Asia as the subspecies *A. a. agrarius*, while populations from Eastern Asia were considered as the subspecies *A. a. ningpoensis*. Several additional subspecies were then proposed in Russia, China and Korea (Gromov and Erbajeva 1995; Koh et al. 1998; Zhang 1997). However, more recent studies based on genetic markers (Atopkin et al. 2007; Koh et al. 2014; Sakka et al. 2010), as well as the findings of the present study, did not indicate any distinction between these subspecies. Our MTCYB gene sequence analyses showed high genetic homogeneity between mainland populations from the Eastern and Western distribution ranges. According to these findings, no subspecies should be recognised within all *A. agrarius* Palaearctic continental populations, including those from China and the Russian Far East. However, Koh et al. (2014) suggested that some differentiation would exist in insular populations from Taiwan and Jeju Island and therefore proposed to consider these insular populations as two different subspecies, *A. a. insulaemus* and *A. a. chejuensis*, respectively. The results of the present study also confirmed the genetic distinctness of these two populations (phylogenetic tree and median-joining network). Further taxonomic investigations are needed to confirm these results.

Conclusion

Our study, using sensitive genetic markers, provides for the first time an overview of the evolutionary and demographic history of the striped field mouse throughout its entire distribution range in the Palaearctic region. Our results suggest that *A. agrarius* is an Asiatic immigrant and a relatively new member of the European fauna. This peculiar phylogeographic pattern highlights the importance of Far East Asian regions as a centre of origin and diversification for several Palaearctic species and as a source for the European biodiversity. This highlights the complexity of the origin of the existing European fauna, where many species have survived in European refugia during the Quaternary glaciations, whereas several others came from much more distant origins.

Acknowledgements We thank Dr. E. Krywko, Dr. Barbara Herzig, Sabrina Schmidt, Ulrike M. Rosenfeld, Nastasja G. Spierling, Denny Maaz, Matthias Wenk, Margrit Bemmann, Jörg Thiel, Eva Ziemssen, Anne Balkema Buschmann, Dan Balkema, Jona Freise, Sandra Blome, Horst Schirrmeier, Anika Hellemann and Mr. Burgemeister for their help in collecting *A. agrarius* material from Poland, Austria and Germany and Sabrina Schmidt, Ulrike M. Rosenfeld, Mathias Schlegel, Dörte Kaufmann, Henrike Gregersen, Sylvia Ferguson, Konrad M. Wanka, Bärbel Hammerschmidt, Christian Kretzschmar, Julie Elkins, Nicole Stieger, Denny Maaz, Fabian Deutskens, Ute Wessels, Grit Möwert, Hanan Sheikh Ali, Nadja Lorenz, Angele Breithaupt, Nastasja G. Spierling, Franziska Thomas, Kathrin Baumann, Annalena Schäfer, Eva Rühe, Theres Wollny, Daniel Windolph, Stephan Drewes and Samuel Petri for dissection of mice and shipment of samples. We thank Michaël Fontaine for his help with the IM analysis. A. Latinne and J.R. Michaux were supported by a Belgian research fellowship from the F.R.S.-FNRS (*Fonds National pour la Recherche Scientifique*) (*mandat "aspirant"* and *"directeur de recherches"*). The EDENext project supported the cost of microsatellite analyses as well as the collection of some specimens included in this study. Specimen collection was also partially supported by the APVV-15-0232 project (to M.S.). Chinese specimens from Ningxia were collected in the framework of the French–Chinese programmes coordinated by P. Giraudoux and supported by the European Union and the US National Institute of Health, Fogarty International Centre.

Compliance with ethical standards

Conflict of interest The authors declare that they have no known competing financial interests or personal relationships that could have appeared to influence the work reported in this paper.

References

Aguilar J-P, Pélissié T, Sigé B, Michaux J (2008) Occurrence of the stripe field mouse lineage (*Apodemus agrarius* Pallas 1771; Rodentia; Mammalia) in the Late Pleistocene of southwestern France. C R Palevol 7:217–225

Andersen LW, Jacobsen M, Vedel-Smith C, Jensen TS (2017) Mice as stowaways? Colonization history of Danish striped field mice. Biol Lett 13:20170064

Atopkin DM, Bogdanov AS, Chelomina GN (2007) Genetic variation and differentiation in striped field mouse *Apodemus agrarius* inferred from RAPD-PCR analysis. Russ J Genet 43:665–676

Bakker ES, Gill JL, Johnson CN, Vera FWM, Sandom CJ, Asner GP, Svenning J-C (2016) Combining paleo-data and modern exclosure experiments to assess the impact of megafauna extinctions on woody vegetation. Proc Natl Acad Sci 113:847–855

Bandelt HJ, Forster P, Rohl A (1999) Median-joining networks for inferring intraspecific phylogenies. Mol Biol Evol 16:37–48

Batuyev AR, Buyantuyev AB, Snytko VA (2000) Geosistemy i kartografirovaniye ekologo-geograficheskikh situatsiy Priselenginskikh kotlovin Baykalskogo regiona [The geosystems and mapping of the ecogeographical situations of the Priselenginsk depressions of the Baikal region]. Novosibirsk

Bazhenov YA, Pavlenko MV, Korablev VP, Kardash AI (2015) Current distribution of the striped field mouse (*Apodemus agrarius* Pallas, 1771) in Eastern Transbaikalia: new findings in the disjunction area. Russ J Biol Invasions 6:1–5

Chapuis MP, Estoup A (2007) Microsatellite null alleles and estimation of population differentiation. Mol Biol Evol 24:621–631

Corbet GB (1978) The mammals of the palaearctic region: a taxonomic review. British Museum (Natural History) and Cornell University Press, London, Ithaca

Deffontaine V, Libois R, KotlÍK P, Sommer R, Nieberding C, Paradis E, Searle JB, Michaux JR (2005) Beyond the Mediterranean peninsulas: evidence of central European glacial refugia for a temperate forest mammal species, the bank vole (*Clethrionomys glareolus*). Mol Ecol 14:1727–1739

Deffontaine V, Ledevin R, Fontaine MC, Quere JP, Renaud S, Libois R, Michaux JR (2009) A relict bank vole lineage highlights the biogeographic history of the Pyrenean region in Europe. Mol Ecol 18:2489–2502

Dietrich W, Katz H, Lincoln SE, Shin HS, Friedman J, Dracopoli NC, Lander ES (1992) A genetic map of the mouse suitable for typing intraspecific crosses. Genetics 131:423–447

Erbajeva MA, Khenzykhenova FI, Alexeeva NV (2013) Aridization of the Transbaikalia in the context of global events during the Pleistocene and its effect on the evolution of small mammals. Quat Int 284:45–52

Evanno G, Regnaut S, Goudet J (2005) Detecting the number of clusters of individuals using the software STRUCTURE: a simulation study. Mol Ecol 14:2611–2620

Excoffier L, Lischer HEL (2010) Arlequin suite ver 3.5: a new series of programs to perform population genetics analyses under Linux and Windows. Mol Ecol Res 10:564–567

Fedorov VB, Goropashnaya AV, Boeskorov GG, Cook JA (2008) Comparative phylogeography and demographic history of the wood lemming (*Myopus schisticolor*): implications for late Quaternary history of the taiga species in Eurasia. Mol Ecol 17:598–610

Fischer S, Mayer-Scholl A, Imholt C, Spierling NG, Heuser E, Schmidt S, Reil D, Rosenfeld UM, Jacob J, Nöckler K, Ulrich RG (2018) *Leptospira* genomospecies and sequence type prevalence in small mammal populations in Germany. Vector-Borne Zoonotic Dis 18:188–199

Fletcher WJ, Sánchez Goñi MF, Allen JRM, Cheddadi R, Combourieu-Nebout N, Huntley B, Lawson I, Londeix L, Magri D, Margari V, Müller UC, Naughton F, Novenko E, Roucoux K, Tzedakis PC (2010) Millennial-scale variability during the last glacial in vegetation records from Europe. Quat Sci Rev 29:2839–2864

Fontaine MC, Tolley KA, Michaux JR, Birkun A, Ferreira M, Jauniaux T, Llavona Á, Öztürk B, Öztürk AA, Ridoux V, Rogan E, Sequeira M, Bouquegneau J-M, Baird SJE (2010) Genetic and historic evidence for climate-driven population fragmentation in a top cetacean predator: the harbour porpoises in European water. Proc R Soc B Biol Sci 277:2829–2837

Gajda E, Hildebrand J, Sprong H, Buńkowska-Gawlik K, Perec-Matysiak A, Coipan EC (2017) Spotted fever rickettsiae in wild-living rodents from south-western Poland. Parasites Vectors 10:413

Gortat T, Rutkowski R, Gryczynska-Siemiatkowska A, Kozakiewicz A, Kozakiewicz M (2013) Genetic structure in urban and rural populations of *Apodemus agrarius* in Poland. Mamm Biol Zeitschrift für Säugetierkunde 78:171–177

Goudet J (2001) FSTAT, a program to estimate and test gene diversities and fixation indices (version 2.9.3). http://www.unil.ch/izea/softwares/fstat.html. Updated from Goudet (1995)

Gromov I, Erbajeva M (1995) The mammals of Russia and adjacent territories; lagomorphs and rodents, vol 167. Russian Academy of Science, Zoological Institute, St Petersburg, p 529

Guindon S, Dufayard JF, Lefort V, Anisimova M, Hordijk W, Gascuel O (2010) New algorithms and methods to estimate maximum-likelihood phylogenies: assessing the performance of PhyML 3.0. Syst Biol 59:307–321

Hall TA (1999) BioEdit: a user-friendly biological sequence alignment editor and analysis program for Windows 95/98/NT. Nucl Acids Symp Ser 41:95–98

Hasegawa M, Kishino H, Yano T-A (1985) Dating of the human-ape splitting by a molecular clock of mitochondrial DNA. J Mol Evol 22:160–174

Herman JS, Paupério J, Alves PC, Searle JB (2014) Land bridge calibration of rates of molecular evolution in a widespread rodent. In: Pontarotti P (ed) Evolutionary biology: genome evolution, speciation, coevolution and origin of life. Springer International Publishing, Berlin, pp 69–86

Herman JS, Jóhannesdóttir F, Jones EP, McDevitt AD, Michaux JR, White TA, Wójcik JM, Searle JB (2016) Post-glacial colonization of Europe by the wood mouse, Apodemus sylvaticus: evidence of a northern refugium and dispersal with humans. Biol J Linn Soc 120(2):313–332

Hewitt GM (2000) The genetic legacy of the Quaternary ice ages. Nature 405:907–913

Hey J, Nielsen R (2004) Multilocus methods for estimating population sizes, migration rates and divergence time, with applications to the divergence of *Drosophila pseudoobscura* and *D. persimilis*. Genetics 167:747–760

Hudson RR (2002) Generating samples under a Wright–Fisher neutral model of genetic variation. Bioinformatics 18:337–338

Hughes ALC, Gyllencreutz R, Lohne ØS, Mangerud J, Svendsen JI (2016) The last Eurasian ice sheets—a chronological database and time-slice reconstruction, DATED-1. Boreas 45:1–45

Kartavtseva IV, Pavlenko MV (2000) Chromosomal variability of the field mouse *Apodemus agrarius* (Rodentia, Muridae). Genetika 36:223–236

Kim HR, Park YC (2015) Genetic diversity and genetic structure of the striped field mouse *Apodemus agrarius coreae* (Muridae, Rodentia) in Korea. Gene 572:292–297

Klempa B, Avsic-Zupanc T, Clement J, Dzagurova TK, Henttonen H, Heyman P, Jakab F, Kruger DH, Maes P, Papa A, Tkachenko EA, Ulrich RG, Vapalahti O, Vaheri A (2013) Complex evolution and epidemiology of Dobrava-Belgrade hantavirus: definition of genotypes and their characteristics. Arch Virol 158:521–529

Kocher TD, Thomas WK, Meyer A, Edwards SV, Pääbo S, Villablanca FX, Wilson AC (1989) Dynamics of mitochondrial DNA evolution in animals: amplification and sequencing with conserved primers. Proc Natl Acad Sci 86:6196–6200

Koh HS, Csorba G, Tiunov MP, Tikhonova G (1998) Morphometric analyses of the three subspecies of striped field mouse, *Apodemus agrarius* Pallas (Mammalia: Rodentia) from Far Eastern Asia: taxonomix status of North Korean striped field mice. Korean J Syst Zool 14:327–334

Koh HS, Shaner PJ, Csorba G, Wang Y, Jang KH, Lee JH (2014) Comparative genetics of *Apodemus agrarius* (Rodentia: Mammalia) from insular and continental Eurasian populations: cytochrome b sequence analyses. Acta Zool Acad Sci Hung 60:73–84

Kopelman NM, Mayzel J, Jakobsson M, Rosenberg NA, Mayrose I (2015) Clumpak: a program for identifying clustering modes and packaging population structure inferences across K. Mol Ecol Res 15:1179–1191

Kraljik J, Paziewska-Harris A, MiklisovÁ D, Blaňarová L, Mošanský L, Bona M, Stanko M (2016) Genetic diversity of *Bartonella* genotypes found in the striped field mouse (*Apodemus agrarius*) in Central Europe. Parasitology 143:1437–1442

Lalis A, Leblois R, Liefried S, Ouarour A, Reddy Beeravolu C, Michaux J, Hamani A, Denys C, Nicolas V (2016) New molecular data favour an anthropogenic introduction of the wood mouse (*Apodemus sylvaticus*) in North Africa. J Zool Syst Evol Res 54:1–12

Lorenzini R, Garofalo L, Qin X, Voloshina I, Lovari S (2014) Global phylogeography of the genus *Capreolus* (Artiodactyla: Cervidae), a Palaearctic meso-mammal. Zool J Linn Soc 170:209–221

Makova KD, Patton JC, Krysanov EY, Chesser RK, Baker RJ (1998) Microsatellite markers in wood mouse and striped field mouse (genus *Apodemus*). Mol Ecol 7:247–255

Michaux JR, Magnanou E, Paradis E, Nieberding C, Libois R (2003) Mitochondrial phylogeography of the Woodmouse (*Apodemus sylvaticus*) in the Western Palearctic region. Mol Ecol 12:685–697

Navascués M (2017) microsatABC-IM: Approximate Bayesian computation inferences under the isolation with migration model from microsatellite data (Version v1.0). Zenodo

Neumann K, Michaux JR, Maak S, Jansman HAH, Kayser A, Mundt G, Gattermann R (2005) Genetic spatial structure of European common hamsters (*Cricetus cricetus*)—a result of repeated range expansion and demographic bottlenecks. Mol Ecol 14:1473–1483

Okulova NM, Duvanova IA, Kalinkina EV, Mironova TA, Nedosekin VY, Drozdova VF (2012) On the ecology of striped field mouse (*Apodemus agrarius* Pall., 1771) in forest-steppes of the chernozem zone: 1. Abund Biol Bull 39:809–815

Pereverzeva VV, Primak AA, Pavlenko MV, Dokuchaev NE, Evdokimova AA (2017) Genetic features and the putative sources of formation of isolated populations of the striped field mouse *Apodemus agrarius* Pallas, 1771 in Magadan oblast. Russ J Biol Invasions 8:87–100

Popov V (2017) A Pleistocene record of *Apodemus agrarius* (Pallas, 1771) (Mammalia: Rodentia) in the Magura Cave, Bulgaria. Acta Zool Bulg 69:121–124

Posada D (2008) jModelTest: Phylogenetic model averaging. Mol Biol Evol 25:1253–1256

Pritchard JK, Stephens M, Donnelly P (2000) Inference of population structure using multilocus genotype data. Genetics 155:945–959

Pudlo P, Marin J-M, Estoup A, Cornuet J-M, Gautier M, Robert CP (2016) Reliable ABC model choice via random forests. Bioinformatics 32:859–866

Raynal L, Marin J-M, Pudlo P, Ribatet M, Robert CP, Estoup A (2019) ABC random forests for Bayesian parameter inference. Bioinformatics 35:1720–1728

Rousset F (2008) GENEPOP ' 007: a complete re-implementation of the GENEPOP software for Windows and Linux. Mol Ecol Res 8:103–106

Ruiz-González A, Madeira MJ, Randi E, Abramov AV, Davoli F, Gómez-Moliner BJ (2013) Phylogeography of the forest-dwelling European pine marten (*Martes martes*): new insights into cryptic northern glacial refugia. Biol J Linn Soc 109:1–18

Sakka H, Quere JP, Kartavtseva I, Pavlenko M, Chelomina G, Atopkin D, Bogdanov A, Michaux J (2010) Comparative phylogeography of four *Apodemus* species (Mammalia: Rodentia) in the Asian Far East: evidence of Quaternary climatic changes in their genetic structure. Biol J Linn Soc 100:797–821

Sheremetyeva IN, Kartavtseva IV, Pavlenko MV, Kostenko VA, Sheremetyev IS, Katin IO, Kosoy ME (2017) Morphological and genetic variability in small island populations of the striped field mouse *Apodemus agrarius* Pallas, 1771. Biol Bull 44:159–171

Sibiryakov PA, Tovpinets NN, Dupal TA, Semerikov VL, Yalkovskaya LE, Markova EA (2018) Phylogeography of the Common Vole *Microtus arvalis*, the Obscurus Form (Rodentia, Arvicolinae): New Data on the Mitochondrial DNA Variability. Russ J Genet 54:1185–1198

Spitzenberger F, Engelberger S (2014) A new look at the dynamic western distribution border of *Apodemus agrarius* in Central Europe (Rodentia: Muridae). Lynx Ser Nova 45:69–79

Stewart JR, Dalén L (2008) Is the glacial refugium concept relevant for northern species? A comment on Pruett and Winker 2005. Clim Change 86:19–22

Suzuki H, Filippucci MG, Chelomina GN, Sato JJ, Serizawa K, Nevo E (2008) A biogeographic view of *Apodemus* in Asia and Europe inferred from nuclear and mitochondrial gene sequences. Biochem Genet 46:329–346

Suzuki Y, Tomozawa M, Koizumi Y, Tsuchiya K, Suzuki H (2015) Estimating the molecular evolutionary rates of mitochondrial genes referring to Quaternary ice age events with inferred population expansions and dispersals in Japanese *Apodemus*. BMC Evol Biol 15:187

Velichko AA (2009) Paleoclimates and Paleoenvironments of Extratropical Area of the Northern Hemisphere. Late Pleistocene-Holocene. GEOS Publishers, Moscow

Xiao H, Tong X, Huang R, Gao L, Hu S, Li Y, Gao H, Zheng P, Yang H, Huang ZYX, Tan H, Tian H (2018) Landscape and rodent community composition are associated with risk of hemorrhagic fever with renal syndrome in two cities in China, 2006–2013. BMC Infect Dis 18:37

Yasuda SP, Vogel P, Tsuchiya K, Han S-H, Lin L-K, Suzuki H (2005) Phylogeographic patterning of mtDNA in the widely distributed harvest mouse (*Micromys minutus*) suggests dramatic cycles of range contraction and expansion during the mid- to late Pleistocene. Can J Zool 83:1411–1420

Zhang Y (1997) Distribution of mammalian species in China. China Forestry Publishing, Beijing

Zhang H, Yan J, Zhang G, Zhou K (2008) Phylogeography and Demographic History of Chinese Black-Spotted Frog Populations (*Pelophylax nigromaculata*): Evidence for Independent Refugia Expansion and Secondary Contact. BMC Evol Biol 8:21

Affiliations

Alice Latinne[1,2] · Miguel Navascués[3,4] · Marina Pavlenko[5] · Irina Kartavtseva[5] · Rainer G. Ulrich[6] · Marie-Laure Tiouchichine[1] · Gilles Catteau[1] · Hela Sakka[1] · Jean-Pierre Quéré[3] · Galina Chelomina[5] · Aleksey Bogdanov[7] · Michal Stanko[8] · Lee Hang[9] · Karsten Neumann[10] · Heikki Henttonen[11] · Johan Michaux[1,12]

1 Laboratoire de génétique de la conservation, Institut de Botanique, Boulevard du rectorat, 27, 4000 Liège, Belgium

2 EcoHealth Alliance, New York, NY 10001, USA

3 CBGP, Univ Montpellier, CIRAD, INRA, IRD, Montpellier SupAgro, Montpellier, France

4 Institut de Biologie Computationnelle, Montpellier, France

5 Federal Scientific Center of the East Asia Terrestrial Biodiversity, Far East Branch of Russian Academy of Sciences, Vladivostok 690022, Russia

6 Friedrich-Loeffler-Institut, Federal Research Institute for Animal Health, Institute of Novel and Emerging Infectious Diseases, Südufer 10, 17493 Greifswald, Insel Riems, Germany

7 Institute of Developmental Biology RAS, Vavilov Str., 26, 119334 Moscow, Russia

8 Institute of Parasitology, Slovak Academy of Sciences, Hlinkova 3, 04001 Košice, Slovakia

9 Program for Veterinary Science, Seoul National University, Seoul, South Korea

10 Institute of Pathology, City Hospital Dessau, Auenweg 38, 06847 Dessau-Roßlau, Germany

11 Natural Resources Institute Finland, POB 9, 00790 Helsinki, Finland

12 Laboratoire de génétique de la conservation, Institut de Botanique, Chemin de la Vallée, 4, 4000 Liège, Belgium